Development of a high-spectral-resolution cadmium zinc telluride pixel detector for astrophysical applications

Fiona A. Harrison, Aleksey E. Bolotnikov, C. M. Hubert Chen, Walter R. Cook, Peter H. Mao, et al.

Fiona A. Harrison, Aleksey E. Bolotnikov, C. M. Hubert Chen, Walter R. Cook, Peter H. Mao, Steven M. Schindler, "Development of a high-spectral-resolution cadmium zinc telluride pixel detector for astrophysical applications," Proc. SPIE 4851, X-Ray and Gamma-Ray Telescopes and Instruments for Astronomy, (11 March 2003); doi: 10.1117/12.461165

SPIE.

Event: Astronomical Telescopes and Instrumentation, 2002, Waikoloa, Hawai'i, United States

Development of a high spectral resolution cadmium zinc telluride pixel detector for astrophysical applications

F. A. Harrison, A. Bolotnikov,
C. M. H. Chen, W. R. Cook, P. H. Mao, S. M. Schindler

Space Radiation Laboratory, 220-47
Division of Physics, Mathematics and Astronomy
Caltech, Pasadena, CA 91125

ABSTRACT

Over the last six years, we have been developing imaging Cadmium Zinc Telluride pixel detectors optimized for astrophysical focusing hard X-ray telescopes. This application requires sensors with modest area ($\sim$ 2cm $\times$ 2 cm), relatively small ($\lesssim 500\mu$m) pixels and sub-keV energy resolution. For experiments operating in satellite orbits, energy thresholds of $\sim 1-2$ keV are also desirable. In this paper we describe the desired detector performance characteristics, and report on the status of our development effort. In particular, we present results from a 1152-channel custom low-noise VLSI readout designed to achieve excellent spectral resolution and good imaging performance in the 5 – 100 keV band.

1. INTRODUCTION

The recent development of depth-graded multilayer optics (e.g. Christensen *et al.* 2000) will enable large-area focusing telescopes to be employed in the hard X-ray band, from five to several hundred keV, for the first time. A number of balloon experiments, as well as future space missions, are currently being planned which will incorporate this technology to achieve an unprecedented combination of sensitivity, angular resolving power, and spectral capability at these energies.

Many of these experiments require focal plane sensors with performance significantly improved compared to existing detectors commonly employed in this band (e.g. imaging alkali halide systems or proportional counters). Achieving the target scientific goals requires focal plane systems with $\sim 500\mu$m spatial resolution, sub-keV energy resolution, and good imaging efficiency from a few to a few hundred keV.

Our group at the Caltech Space Radiation Laboratory has been developing solid state CdZnTe pixel sensors designed for two hard X-ray focusing experiments experiments: The *High-Energy Focusing Telescope (HEFT)* and the *Constellation-X* Hard X-ray Telescope (HXT). We have optimized these detectors for spectral resolution, imaging performance, and low-energy threshold. In this paper we describe the required sensor performance, and the associated detector technical parameters. Section 3 describes the architecture of the sensor architecture, and Section 4 presents performance results to-date. Finally, we describe our plans for future effort.

2. FOCAL PLANE SENSOR PERFORMANCE REQUIREMENTS

Table 1 summarizes the desirable performance characteristics for the *HEFT* and *Con-X* focal plane sensors. Both have worst-case angular resolution goals of 1 $'$. The *HEFT* energy band extends from the atmospheric cutoff of $\sim$20 keV at the low end to 100 keV, in order to cover the radioactive decay lines from ^{44}Ti at 68 and 78 keV. Because the *HEFT* scientific goals include spectroscopy of nuclear lines and cyclotron features in high magnetic field pulsars, the spectral resolution goal is aggressive – better than 1 keV FWHM at the ^{44}Ti line energies. The *Con-X* HXT is emphasizing continuum observations at lower energy. Although the fractional resolution requirement is less stringent, the desire to operate at low energies (5 keV) places a requirement for low noise, similar to that for *HEFT*, on the detector.

Further author information: (Send correspondence to Fiona A. Harrison)
E-mail: fiona@srl.caltech.edu

X-Ray and Gamma-Ray Telescopes and Instruments for Astronomy, Joachim E. Trümper, Harvey D. Tananbaum, Editors, Proceedings of SPIE Vol. 4851 (2003)

Parameter	*HEFT*	*Con-X* HXT
energy band	$20-100$ keV	$<5->40$ keV ($1-60$ goal)
FOV	$10'$ (50 keV)	$\geq 8'$ ($6-40$ keV)
angular resolution	$1'$	$<1'$ ($30''$ goal)
collecting area	200 cm^2 (50 keV)	1500 cm^2 (40 keV)
energy resolution (FWHM)	<1 keV (68 keV)	<1.2 keV (6 keV)

Table 1. *HEFT* and *Con-X* performance goals.

Table 2 shows the telescope parameters for these two experiments, along with the sensor requirements associated with the performance goals for the telescopes as currently designed. Although the bandpass and fractional spectral resolution requirements differ, both instruments require a very low level of electronic noise. For *HEFT* this is to achieve good spectral resolution, and for *Con-X* it allows a threshold at low X-ray energies. The detector and pixel dimensions are also similar, in spite of the different telescope focal lengths, due to the somewhat smaller FOV and more aggressive angular resolution goal of *Con-X*.

Parameter	*HEFT*	*Con-X* HXT
Telescope parameters		
focal length	6 m	10 m
optics	conical approx. Wolter I (12 modules)	Wolter I or approx. (9 modules)
Sensor requirements		
pixel size ($1/3 \times \Delta\theta \times f$	580μm	480 μm
energy band	$20-100$ keV	5 - 60 keV
energy resolution (FWHM)	<1 keV (68 keV)	<1.2 keV (6 keV)
dimensions (FOV $\times f$)	2.1×2.1 cm	2.3×2.3 cm
quantum efficiency	$>90\%$ ($20-100$ keV)	$>90\%$ ($6-60$ keV)
trigger required	yes	yes
maximum countrate	100 ct/s/pixel	100 ct/s/pixel
	500 ct/s/module	500 ct/s/module
typical countrate	few ct/s/module	few ct/s/module
time resolution	10μs	10 μs

Table 2. Telescope parameters and sensor requirements for *HEFT* and *Con-X*.

3. CDZNTE PIXEL DETECTOR DESIGN

We have developed a CdZnTe pixel sensor and a custom low-noise VLSI readout designed to meet the *HEFT* and *Con-X* requirements described above. Fig. 1 shows the basic focal plane architecture. A CdZnTe sensor with the anode side segmented into contacts is indium bump bonded to the VLSI readout, where each pixel is connected to a separate readout chain (the combination being called a hybrid). Each sensor element is 1.3 cm $\times$2.5 cm on a side (limited by the availability of large, uniform CdZnTe and the VLSI reticle size). To fill the focal plane, we will tile two hybrids side-by-side, minimizing the gap in between to the extent possible. Table 3 summarizes the characteristics of the hybrid.

Pixel design. The goals in designing the CdZnTe pixel contacts are to minimize the size, while at the same time avoiding significant charge loss for events occuring at the pixel edges. The input capacitance is dominated by the pixel contact-to-VLSI ground-plane capacitance, so reducing the contact size directly reduces the electronic noise. Charge-loss between pixels occurs when charge reaches the low-field region occuring in the gap between pixel contacts, where it becomes trapped.[2]

The severity of the charge loss depends on the electric field geometry, which is determined not only by the contact and gap size, but also by the ratio of bulk to surface conductivity. The higher the surface conductance relative to the

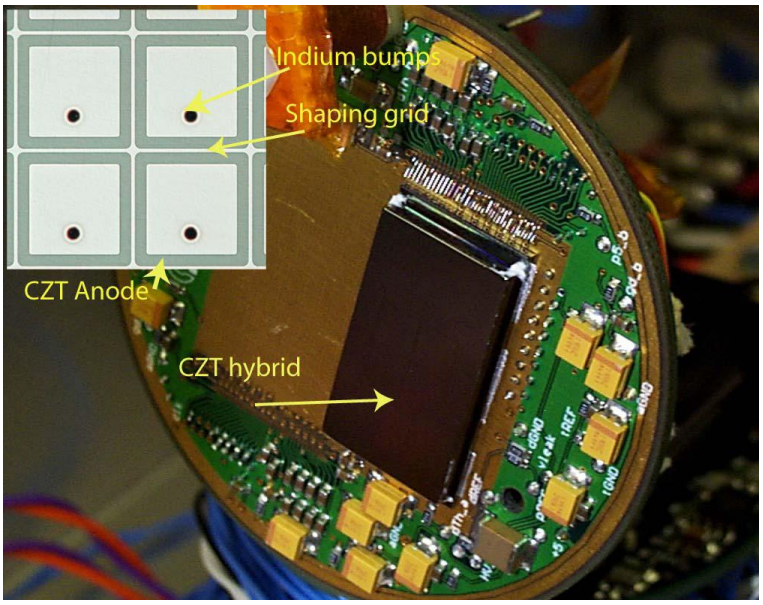

Figure 1. *Photo of a* HEFT *hybrid detector mounted to the motherboard. Two detectors,* 1.3×2.5 *cm each, comprise the focal plane of each focusing telescope. The insert shows the anode (bottom side) of the CdZnTe.*

pixel size	500 μm	contact dimension	450 μm
hybrid size	1.3×2.5cm	typ bias	300 V
grid thickness	15 μm	gap width	17.5 μm
CdZnTe thickness	2 mm	typ grid–contact bias	4 V
operating temp.	-10 – -20°C	power/pixel	50μW

Table 3. CdZnTe hybrid parameters.

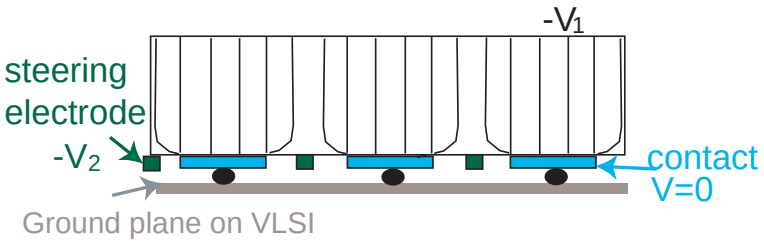

Figure 2. *Diagram of the hybrid electrode geometry.*

bulk, the greater the fraction of field lines that terminate in the gaps. If there is no electric field component parallel to the surface, the charge reaching the gap will not be directed toward the anode.

Because of the above effects, we are employing a three-terminal design for the pixel contact in order to minimize contact size yet avoid significant inter-pixel charge loss (see Figure 2). We include thin strips between the square pixel contacts, held at a potential intermediate between the cathode and anode. This "grid" increases the electric field component on and parallel to the detector surface (see Bolotnikov *et al.* (2000) for details). The disadvantage of the grid is that grid-pixel leakage current dominates the total detector leakage if the grid for typical operating potentials. The surface resistivity is difficult for the manufacturer (eV Products of Saxenberg, PA) to control, and the leakage current can dominate the total detector noise in some devices, particularly if operated near room temperature. Typical total leakage currents are $\lesssim 100$ pA/pixel for sensors we accept for use in a hybrid.

Readout architecture. We have developed a custom, low-noise CMOS readout for *HEFT* and *Con-X*. This device, designed at Caltech's Space Radiation Laboratory, has a separate readout chain for each pixel, where all pixel-specific circuitry fits within a 500μm square.

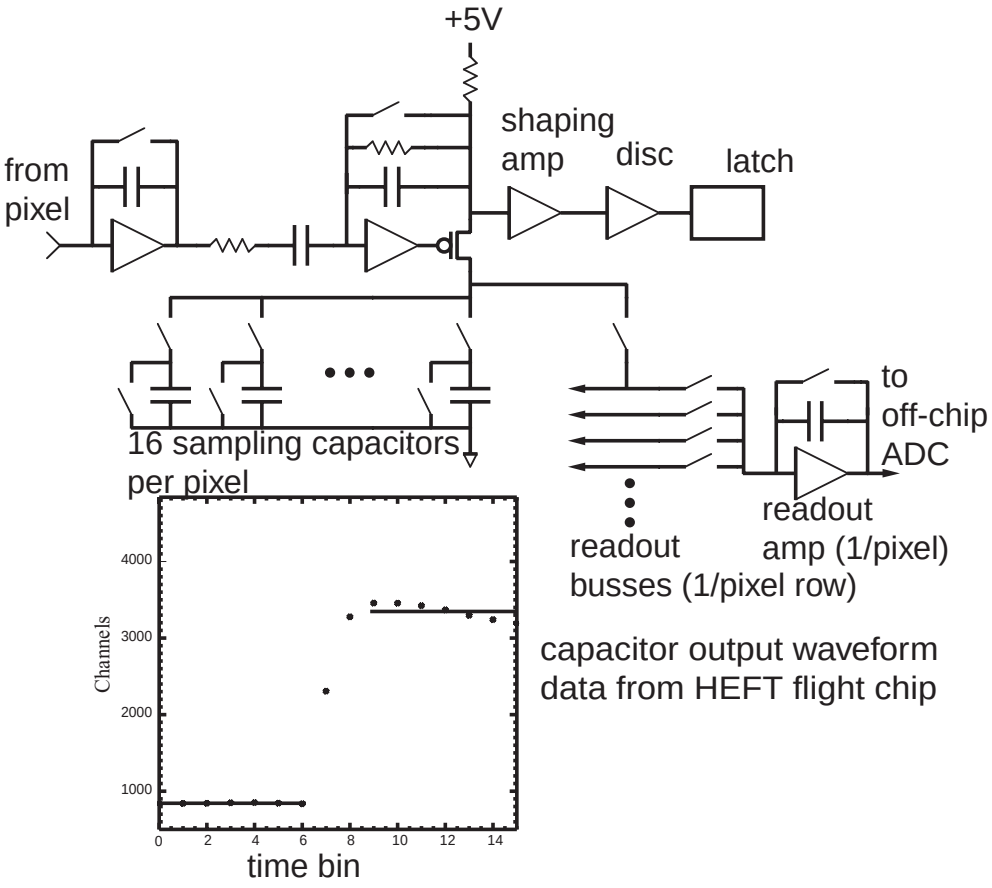

Figure 3. *Schematic of the low-noise custom VLSI pixel readout. The insert shows the output of the 16 sampling capacitors as obtained from the flight chip.*

The circuitry for each pixel contains a preamplifier, a postamplifier, a bank of 16 sampling capacitors, a shaping amplifier, a discriminator and a latch (Figure 3). The postamp output is a current signal having a tail pulse shape with 100 ns rise and 30 μs fall time constants. While awaiting a detector signal pulse the postamplifier current output is steered from one capacitor to the next, such that the sampling capacitor bank stores a continuously updated history

of the postamplifier output waveform. After a signal pulse is detected by any discriminator, the waveform sampling continues for 8 more sampling periods (typically 1 μs each) then sampling stops with approximately 7 pre-trigger samples, 1 intermediate sample and 8 post-trigger samples (Figure 3).

The design allows for flexible readout of selected pixels. An off-chip co-processor determines which pixels were triggered. Typically either a single or two adjacent pixels trigger, and we read out those as well as the surrounding ones. During the analog readout process, stored charges are routed sequentially to a precision on-chip readout amplifier which drives an off-chip 12-bit ADC. We use a simple digital algorithm to extract the energy from each 16 sample waveform, weighting the various samples for optimum noise performance. The readout of untriggered surrounding pixels allows the sensitive detection of events in which the signal has split between pixels and the reconstruction of the total event energy for such events.

In the chip, digital signals operate continuously without perturbing the sensitive analog circuits nearby. Systematic noise due to the coupling of digital signals into analog signal processing paths is well below the limits imposed by thermal noise.

4. DETECTOR AND READOUT PERFORMANCE

We have verified the operation of the VLSI and CdZnTe sensor independently, and also together in a bonded hybrid. To-date, we have tested a single hybrid both with test pulses, as well as gamma-ray illumination of individual pixels, and measurement of charge collection between pixels (Figure 5). These test results indicate that the chip functions well, and that when operated at 10°C, the hybrid can meet the spectral resolution requirements, however additional work is required to achieve the low-energy threshold required by *Constellation-X*.

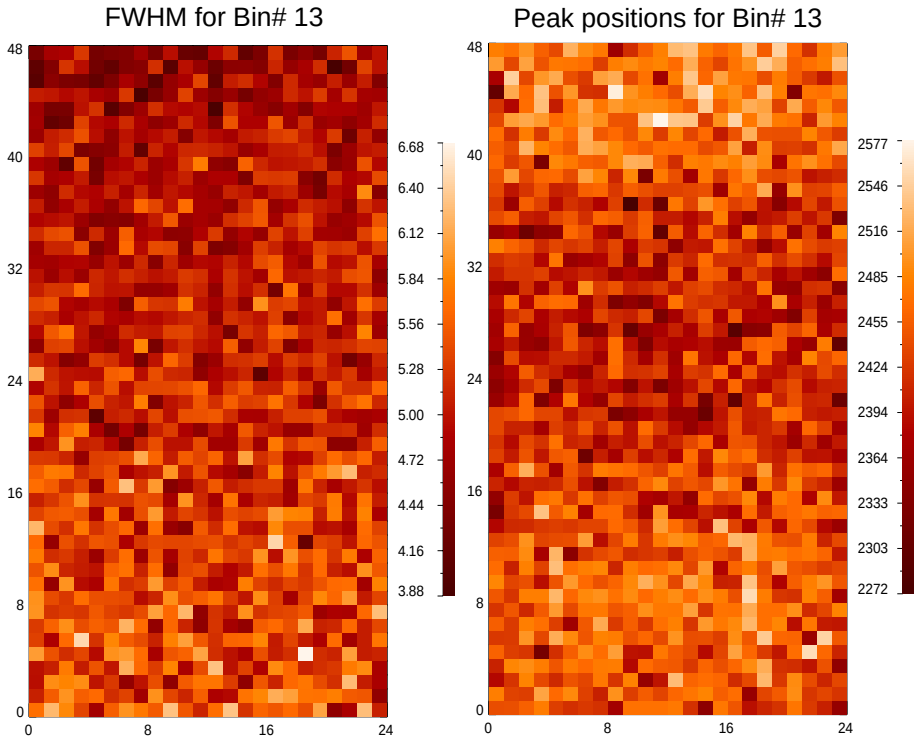

Figure 4. *FWHM noise (in channels) and peak position for all pixels in a flight ASIC, as measured using an on-chip test pulse. The figure demonstrates the uniform response and 300 eV FWHM average noise performance (with no sensor attached).*

Figure 4 shows the response of the full, flight VLSI chip to on-chip test-pulse stimulation. The FWHM noise has an average value of 300 eV FWHM, with a standard deviation of about 10%. The figure also shows the gain uniformity of the chip (right panel). The average gain variations are 2% , with maximum excursions from the average

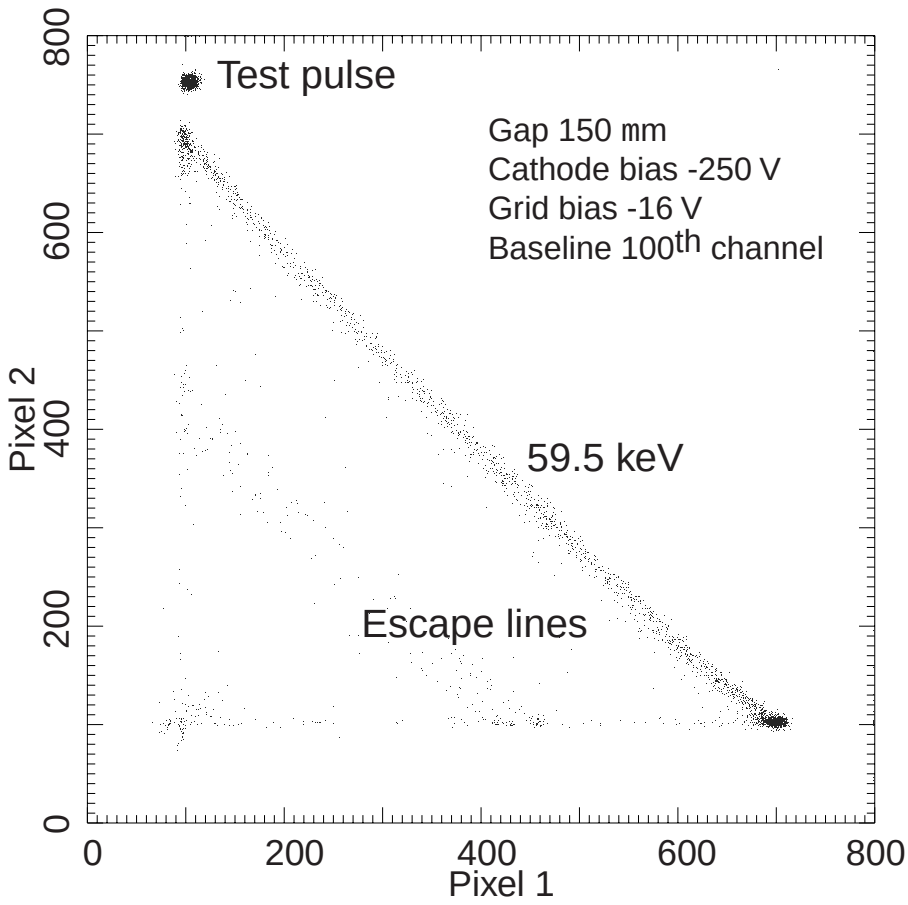

Figure 5. *Signal on two adjacent pixels for events collimated and aimed between two pixels. The minimal curvature in the line indicates that charge collection is nearly complete even for events split between pixels.*

of 5.5% . Connection of the detector adds 280 fF of capacitance to the input, increasing the measured noise to an average value of 620 eV.

To-date we have also tested the response of one hybrid detector to gamma-radiation. Due to problems encountered in the Indium bump bonding of this device, only $\sim 60\%$ of the pixels were connected to the readout. In addition, due to limitations of the software controlling the chip, we did not operate the chip in the final mode where random individual triggers will be identified and read by the processor. Rather, we read triggers only from selected pixels under study. Nevertheless, we were able to characterize the device spectral resolution.

Figure 6 shows an ^{241}Am spectrum taken at 10° C, with the source collimated to the center of an single pixel. The 620 eV test pulser width is largely due to electronic noise, the contribution from leakage current for this device at this temperature being small in comparison. We measure a FWHM resolution of 0.9 keV for the 60 keV line.

5. FUTURE PLANS

Our measurements so-far have been largely on single-pixels, and a priority is to investigate further the resolution of the device once events split between pixels are included. We have now fabricated a second device with $> 90\%$ of the pixels connected, and we plan to test these to quantify residual inter-pixel charge loss. If this can be adequately characterized, the effect can be mitigated to some extent by correcting the pulse heights as a function of the ratio of charge on adjacent pixels.

We are also investigating packaging techniques aimed at reducing the contact-ground plane capacitance. Specifically, we are currently fabricating a test device with an interposing epoxy layer aimed at increasing the sensor to

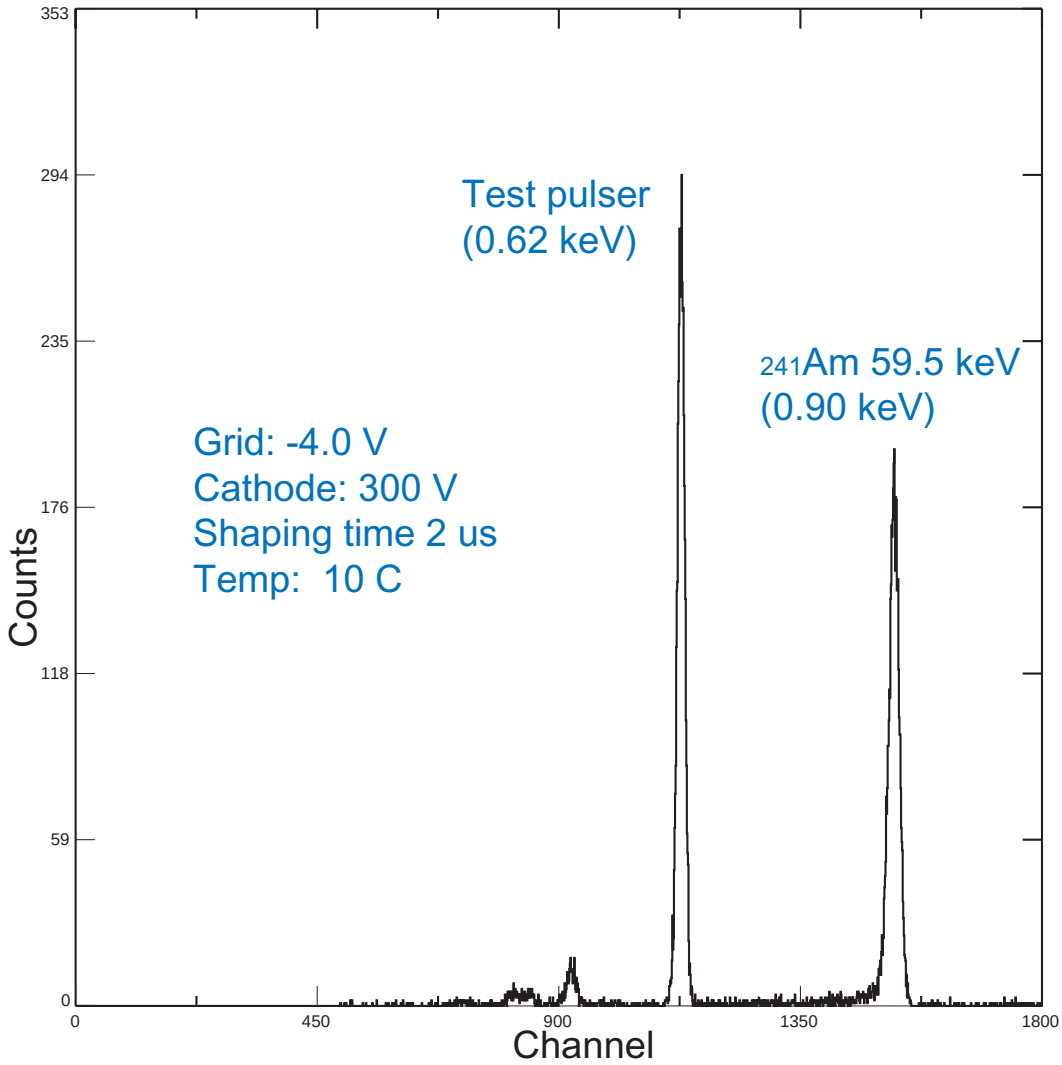

Figure 6. *Measured spectrum of a ^{241}Am source collimated to a single pixel of a a hybrid detector operated at 10° C. The total FWHM noise is 0.9 keV. The tallest peak is from an on-chip test pulser.*

VLSI spacing by a factor of 5 relative to the $\sim 15\mu$m we currently achieve with Indium bonding. This will reduce the input capacitance, and therefore the electronic noise, substantially.

Finally, we plan detailed characterization of the detection threshold across the chip. Currently, we get retriggering of the device for thresholds below ~8 keV. This will limit the reconstruction of split-pixel events to a factor 2 or more above this. It is possible that better shielding of the current device will enable us to reduce this with the current layout.

6. CONCLUSION

The excellent resolution and low electronic noise achieved with our prototype devices show that the *HEFT* and *Con-X* sensor performance goals can be achieved with CdZnTe pixel detectors. The material uniformity is sufficient to avoid severe imperfections for the sizes employed in these applications, the leakage current and electronic noise levels are low enough, and the charge trapping effects negligible enough that sub-keV spectral resolution goal can be exceeded. Further work, however, remains to fully demonstrate the imaging performance (reconstruction of multiple-pixel events), and to show that dead area between hybrids can be maintained at an acceptable level. In addition, we must reduce the electronic threshold, currently dominated by systematic effects, in order to achieve the desired threshold for events split between pixels.

7. ACKNOWLEDGEMENTS

This work is supported in part by NASA's SR&T program (NAGW 5-5289). FAH acknowledges support from a Presidential Early Career Award. We thank Jill Burnham and Branislav Kecman for their contributions to the detector bonding and VLSI development.

REFERENCES

1. F. E. Christensen, J. M. Chakan, W. W. Craig, C. J. Hailey, F. A. Harrison, V. Honkimaki, M. Jimenz-Garate, P. H. Mao, D. L. Windt, and E. Ziegler, "Measured reflectance of graded multilayer mirrors designed for astronomical hard x-ray telescopes," *Nuc.Inst.Meth.* **in press**, 2000.
2. A. E. Bolotnikov, W. R. Cook, F. A. Harrison, A.-S. Wong, S. M. Schindler, and A. C. Eichelberger, "Charge loss between contacts of cdznte pixel detectors," *Nuc. Inst. Meth. A* **432**, p. 326, 1999.
3. A. E. Bolotnikov, S. E. Boggs, W. R. Cook, C. H. Chen, F. A. Harrison, and S. M. Schindler these proceedings, 2000.